## SUPPLEMENTARY NOTES

### Supplementary Note 1: Uhlmann phase for qubit systems

The Uhlmann phase extends the notion of the geometric Berry phase from pure quantum states (Berry) to mixed quantum states described by density matrices. Uhlmann was first to study this problem from a rigorous mathematical perspective [1] and to find a satisfactory solution [2–5].

Let $\theta(t)|_{t=0}^{1}$ define a trajectory along a family of single qubit density matrices parametrised by $\theta$,

$$\rho_\theta = (1-r)|0_\theta\rangle\langle 0_\theta| + r|1_\theta\rangle\langle 1_\theta|, \tag{S1}$$

where $r$ stands for the degree of mixedness between the ground state $|0_\theta\rangle$ and the excited state $|1_\theta\rangle$. Note that $\rho_\theta$ can always be viewed as a pure state $|\Psi_\theta\rangle$ in an enlarged Hilbert space $\mathcal{H} = \mathcal{H}_\mathrm{S} \otimes \mathcal{H}_\mathrm{A}$, where $S$ stands for system and $A$ for the ancilla degrees of freedom. This process is called purification, and satisfies the constraint $\rho_\theta = \mathrm{Tr}_\mathrm{A}\Big(|\Psi_\theta\rangle\langle\Psi_\theta|\Big)$. The set of purifications $|\Psi_\theta\rangle$ generates the family of density matrices $\rho_\theta$. This aims to be the density-matrix analog to the standard situation where vector states $|\psi\rangle$ span a Hilbert space and generate pure states by the relation $\rho = |\psi\rangle\langle\psi|$. Actually, the phase freedom of pure states, U(1)-gauge freedom, is generalised to a U($n$)-gauge freedom ($n$ is the dimension of the density matrix). This occurs since $|\Psi_\theta\rangle$ and $V_\mathrm{A}^\mathrm{t}|\Psi_\theta\rangle$ are purifications of the same density matrix for some unitary operator $V_\mathrm{A}^\mathrm{t}$ acting on the ancilla degrees of freedom. The superindex t denotes the transposition with respect to the qubit eigenbasis. If the trajectory defined by $\theta(t)$ is closed $\rho_{\theta(1)} = \rho_{\theta(0)}$, the initial and final purifications must differ only in a unitary transformation $V_\mathrm{A}^\mathrm{t}$, $|\Psi_{\theta(1)}\rangle = V_\mathrm{A}^\mathrm{t}|\Psi_{\theta(0)}\rangle$. Hence, by analogy to the pure state case, Uhlmann defines a parallel transport condition such that $V_\mathrm{A}$ is constructed by imposing that the distance between two infinitesimally closed purifications, $\||\Psi_{\theta(t+dt)}\rangle - |\Psi_{\theta(t)}\rangle\|^2$, reaches its minimum value. Then it is possible to write

$$V_\mathrm{A} = \mathcal{P}\mathrm{e}^{\int A_\mathrm{U}}, \tag{S2}$$

where $\mathcal{P}$ stands for the path ordering operator along the trajectory $\theta(t)|_{t=0}^{1}$, and $A_\mathrm{U}$ is the so-called Uhlmann connection form [1, 6, 7].

The Uhlmann geometric phase is defined from the mismatch between the initial point $|\Psi_{\theta(0)}\rangle$ and the final point after parallel transport, i.e. $|\Psi_{\theta(1)}\rangle$,

$$\Phi_\mathrm{U} := \arg\left[\langle\Psi_{\theta=0}|\Psi_{\theta=1}\rangle\right] = \arg\mathrm{Tr}\left[\rho_{\theta(0)}V_\mathrm{A}\right]. \tag{S3}$$

This phase is a gauge independent quantity [1–3], that comes from the parallel transport of the purification $|\Psi_\theta\rangle$. The most explicit formula for the Uhlmann connection was given by Hübner [4],

$$A_\mathrm{U} = \sum_{i,j} |\psi_\theta^i\rangle \frac{\langle\psi_\theta^i|\left[(\partial_\theta\sqrt{\rho_\theta}), \sqrt{\rho_\theta}\right]|\psi_\theta^j\rangle}{p_\theta^i + p_\theta^j}\langle\psi_\theta^j|d\theta, \tag{S4}$$

in the spectral basis of $\rho_\theta = \sum_j p_\theta^j|\psi_\theta^j\rangle\langle\psi_\theta^j|$. The parameter $\theta$ may play the role of the crystalline momentum in condensed matter systems.

The derivative of the square-root of the density matrix with respect to the transport parameter $\theta$ is given by

$$\begin{aligned}\partial_\theta\sqrt{\rho_\theta} \;&=\; \sqrt{(1-r)}\big(|\partial_\theta 0_\theta\rangle\langle 0_\theta| + |0_\theta\rangle\langle\partial_\theta 0_\theta|\big) + \\ &+\; \sqrt{r}\big(|\partial_\theta 1_\theta\rangle\langle 1_\theta| + |1_\theta\rangle\langle\partial_\theta 1_\theta|\big).\end{aligned} \tag{S5}$$

We can simplify the connection $A_\mathrm{U}$ in Eq. (S4), for the density matrix (S1) and the Hamiltonian (3) in the main text. We substitute Eq. (S5) in Eq. (S4), and take into account that the summation indices in Eq. (S4) only runs over the states $|1_\theta\rangle$ and $|0_\theta\rangle$, obtaining

$$\begin{aligned}A_\mathrm{U} = \Big[&(1-p_r)\langle 1|\partial_\theta 0_\theta\rangle\ |0_\theta\rangle\langle 1_\theta| \\ &+ (1-p_r)\langle 0_\theta|\partial_\theta 1_\theta\rangle\ |0_\theta\rangle\langle 1_\theta|\Big]d\theta,\end{aligned} \tag{S6}$$

where $p_r = 2\sqrt{r(1-r)}$.

For computational purposes, we fix the gauge for the eigenstates of the system Hamiltonian in Eq. (3) such that,

$$|0_\theta\rangle \;=\; \frac{1}{\sqrt{1+g^2(\theta,M)}}\begin{pmatrix}1\\ g(\theta,M)\end{pmatrix}, \tag{S7}$$

$$|1_\theta\rangle \;=\; \frac{1}{\sqrt{1+g^2(\theta,M)}}\begin{pmatrix}g(\theta,M)\\ -1\end{pmatrix}, \tag{S8}$$

where

$$g(\theta,M) := \frac{\sin\theta}{M+\cos\theta+\sqrt{1+M^2+2M\cos\theta}}. \tag{S9}$$

From Eq. (S7) and Eq. (S8), we compute

$$\begin{aligned}\langle 0_\theta|\partial_\theta 1_\theta\rangle = \frac{\partial_\theta n_\theta^x}{2n_\theta^z} \;&=\; \frac{1+M\cos\theta}{2+2M^2+4M\cos\theta}, \\ |0_\theta\rangle\langle 1_\theta| - |1_\theta\rangle\langle 0_\theta| \;&=\; \begin{pmatrix}0 & -1\\ 1 & 0\end{pmatrix},\end{aligned} \tag{S10}$$

where $n_\theta^i$ is the $i-$th component of the winding vector. Finally, we insert Eqs. (S10) in Eq. (S6) and obtain

$$A_\mathrm{U} = -\mathrm{i}(1-p_r)\frac{\partial_\theta n_\theta^x}{2n_\theta^z}\boldsymbol{\sigma}_y d\theta. \tag{S11}$$

As the connection in Eq. (S11) commutes for different values of $\theta$, we can drop the path ordering that appears in the expression for the Uhlmann unitary [Eq. (S2)], and get the simplified equation

$$V_{\mathrm{A}}(\theta) = \mathrm{e}^{-\mathrm{i}(1-p_r)\int_0^\theta \frac{\partial_{\theta'} n^x_{\theta'}}{2n^z_{\theta'}}\boldsymbol{\sigma}_y d\theta'}. \quad \text{(S12)}$$

Lastly, we substitute Eq. (S12) and Eq. (S1) in Eq. (S3) to compute the Uhlmann phase

$$\Phi_{\mathrm{U}} = \arg\left\{\cos\left[\frac{1-2p_r}{2}\int_0^\theta\left(\frac{\partial_{\theta'} n^x_{\theta'}}{n^z_{\theta'}}\right)d\theta'\right]\right\}. \quad \text{(S13)}$$

The mapping $\rho \longrightarrow V_{\mathrm{A}}$ is a so-called pointed holonomy. This means, that even if the trajectory in parameter space is closed, in general the holonomy depends on the initial point of the path [7, 8]. Nonetheless, we have identified instances in which the pointed holonomy reduces to an *absolute holonomy* becoming independent of the initial point [6, 9]. This is indeed the case studied in the present paper, as well as most of the representative models of 1D and 2D topological insulators and superconductors.

### Supplementary Note 2: Holonomic time evolution

At this stage, we would like to physically implement the holonomy that has been mathematically described in the previous section. For that purpose, we express the parallel transport generated by the change in the parameter $\theta$, as a unitary time evolution over system and ancilla $U_{\mathrm{S}} \otimes U_{\mathrm{A}}$ where the control-parameter $\theta(t)$ is varied in time. The system unitary evolution $U_{\mathrm{S}}$ is defined through the relations

$$|0\rangle_{\theta(t)} := U_{\mathrm{S}}(t)|0\rangle, \quad |1\rangle_{\theta(t)} := U_{\mathrm{S}}(t)|1\rangle, \quad \text{(S14)}$$

where $|0\rangle = \begin{pmatrix}1\\0\end{pmatrix}$ and $|1\rangle = \begin{pmatrix}0\\1\end{pmatrix}$ is the standard qubit basis. Using the eigenstate equations (S7) and (S8), $U_{\mathrm{S}}(\theta)$ is obtained straightforwardly,

$$U_{\mathrm{S}}(t) = \frac{1}{\sqrt{1+g^2[\theta(t),M]}}\begin{pmatrix}1 & -g[\theta(t),M]\\ g[\theta(t),M] & 1\end{pmatrix}, \quad \text{(S15)}$$

where $g(\theta, M)$ was defined in Eq. (S9).

At this point Eq. (S15) can be expressed as the exponential of a Hamiltonian using the following relations

$$U_{\mathrm{S}}(t) = \mathrm{e}^{-\mathrm{i}\int_0^t h(t')dt'}, \quad \text{(S16)}$$

$$h(t) = \mathrm{i}\left(\frac{d\theta}{dt}\right)[\partial_\theta U_{\mathrm{S}}(\theta)]U_{\mathrm{S}}^\dagger(\theta). \quad \text{(S17)}$$

We substitute Eq. (S15) into Eq. (S17), arriving at

$$h(t) = \left(\frac{d\theta}{dt}\right)\frac{\partial_{\theta(t)} n^x_{\theta(t)}}{2n^z_{\theta(t)}}\boldsymbol{\sigma}_y, \quad \text{(S18)}$$

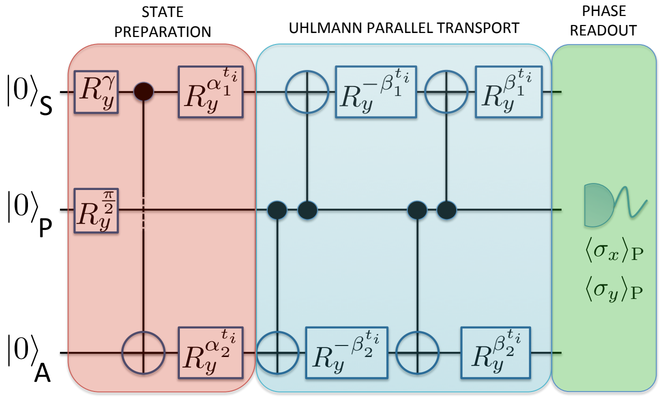


FIG. S1: Circuit diagram to test the Uhlmann parallel transport condition. The gates $R_y^\alpha$ represent single qubit rotations about the y-axis for an angle $\alpha$, and the different angles of rotation are given in Eq. (S21) and Eq. (S22).

where we have used Eq. (S10) as well.

The unitary for the ancilla qubit $U_{\mathrm{A}}$ is determined by combining: 1) the transport of the eigenstates $|0(1)_\theta\rangle$ through $U_{\mathrm{S}}(t)$ and 2) the Uhlmann correction $V_{\mathrm{A}}[\theta(t)]$, for the purification as a whole to be parallely transported [Eq. (S12)]; hence,

$$U_{\mathrm{A}}(t) = [U_{\mathrm{S}}^\dagger(t)V_U(t)]^{\mathrm{t}}. \quad \text{(S19)}$$

Here, the superindex t denotes the transposition with respect to the qubit eigenbasis. Further simplifications of Eq. (S19) using Eq. (S18) and Eq. (S12) lead to

$$U_{\mathrm{A}}(t) = \mathrm{e}^{-\mathrm{i}p_a\int_0^t h(t')dt'}, \quad \text{(S20)}$$

with $p_a = p_r$.

### Supplementary Note 3: Experimental test of Uhlmann parallel transport

In this section we present further details on how to experimentally test the Uhlmann parallel transport condition along the holonomy. The experimental results are shown in the middle plot of Fig. 3 in the main text.

The protocol is depicted in Fig. S1. The state preparation part of the protocol is the same as in the state-dependent and state-independent protocols described in the main text. We prepare the initial state $|\Psi_{t=0}\rangle$ using single qubit rotations $R_y^\theta$ about the y-axis for an angle $\theta$ and a two-qubit controlled not gate. Then, we apply $R_y^{\alpha_1^{t_i}}$ and $R_y^{\alpha_2^{t_i}}$ on the system and ancilla qubits respectively, where

$$\begin{aligned}\alpha_1^{t_i} &= 2\int_0^{t_i} h(t')dt',\\ \alpha_2^{t_i} &= p_r\alpha_1^{t_i}.\end{aligned} \quad \text{(S21)}$$

The entangled state between system and ancilla will evolve until $|\Psi_{t=t_i}\rangle$ (red block of Fig. S1). Next, we apply $R_y^{\beta_{1(2)}^{t_i}}$ to the system and ancilla qubits, conditional on the probe (which has been previously prepared on an equal superposition of states $|0\rangle$ and $|1\rangle$). The angles of rotation in this case are

$$\begin{aligned} \beta_1^{t_i} &= \int_{t_i}^{t_i+\delta t} h(t')dt', \\ \beta_2^{t_i} &= p_r \beta_1^{t_i}. \end{aligned} \tag{S22}$$

This part comprises the blue block in Fig. S1. As a consequence, the three qubits $\{\mathrm{S}, \mathrm{A}, \mathrm{P}\}$ end up in the superposition

$$|\Phi\rangle_{\mathrm{SAP}} = \frac{1}{\sqrt{2}}\big(|\Psi_{t=t_i}\rangle \otimes |0\rangle_P + |\Psi_{t=t_i+\delta t}\rangle \otimes |1\rangle_P\big). \tag{S23}$$

Now we are interested in reading out the relative phase $\Phi$ from the state of the probe qubit. Tracing out the system and ancilla in Eq. (S23), the reduced state for the probe qubit is

$$\begin{aligned} \rho_{\mathrm{P}} = \frac{1}{2}\Big(&\mathbb{1} + \mathrm{Re}(\langle\Psi_{t=t_i}|\Psi_{t=t_i+\delta t}\rangle)\boldsymbol{\sigma}_x \\ &+ \mathrm{Im}(\langle\Psi_{t=t_i}|\Psi_{t=t_i+\delta t}\rangle)\boldsymbol{\sigma}_y\Big). \end{aligned} \tag{S24}$$

Thus, by measuring the expectation values $\langle\boldsymbol{\sigma}_x\rangle$ and $\langle\boldsymbol{\sigma}_y\rangle$ (green block of Fig. S1), we can retrieve the relative phase $\Phi$ between the states $|\Psi_{t=t_i}\rangle$ and $|\Psi_{t=t_i+\delta t}\rangle$. If the transport fulfills the Uhlmann parallel condition between $t_i$ and $t_i+\delta t$, then the two vectors should be in phase $\Phi \approx 0$. This is actually what we observe in the experiment (see the middle plot in Fig. 3 of the main text).

### Supplementary Note 4: Quantum Algorithm

The experiments on the topological Uhlmann phase have been realized on the IBM Quantum Experience (ibmqx2) [11], a quantum computing platform with online user-access based on five fixed-frequency transmon-type qubits coupled via co-planar waveguide resonators. We have used three qubits, qubit Q0 as the probe qubit, Q1 as the system qubit and Q2 as the ancilla qubit. This choice is motivated by the connectivity required for the measurement protocol and the superior $T_1$ and $T_2$ times of this set of qubits when compared to the set $\{Q2, Q3, Q4\}$ at the time of the experiment. We have used the open-source python library *QISKit* [12] to program the quantum computer and retrieve the data. The quantum algorithm to measure the expectation values of $\sigma_x$ is

```
OPENQASM 2.0;
include "qelib1.inc";
qreg q[5];
creg c[5];
u3(θ,0,0) q[1];
cx q[1],q[2];
h q[0];
cx q[0],q[2];
cx q[0],q[1];
barrier q[0],q[1],q[2],q[3],q[4];
u3(β2,0,0) q[2];
u3(β1,0,0) q[1];
barrier q[0],q[1],q[2],q[3],q[4];
cx q[0],q[2];
cx q[0],q[1];
h q[0];
measure q[0] -> c[0];
```

in the *OPENQASM* intermediate representation, described in [13]. For measuring $\sigma_y$ we insert the rotation 'sdg q[0];' before the last hadamard gate 'h [q0]'. The circuit diagram (including the rotation for the measurement of $\sigma_y$) is shown in Figure S2. Note, that we do not implement the last set of single-qubit rotations on system and ancilla qubits because these do not change the outcome of the measurement of the probe qubit $Q_0$. The phase is then extracted from the measured data by evaluating $\Phi_{\mathrm{M}} = \arg(\langle\sigma_x\rangle - i\langle\sigma_y\rangle)$.

### Supplementary Note 5: Interacting Systems & 2D

The protocol to measure the topological Uhlmann phase deals with single-qubit Hamiltonians [Eq. (3) in the main text]. These can be mapped to free-fermion topological insulators. We may identify the ramp parameter $\theta$ with the crystalline momentum in the Brillouin zone $k$. In 2D, a way to define a non-trivial topological invariant for isotropic systems at finite temperature is by means of the winding number of the Uhmann phase, as shown in Refs. [7, 9, 10]. We could test this experimentally by mapping two independent parameters $\theta$ and $\delta$ of our quantum simulator to the crystalline momentum of a 2D topological insulator $k_x$ and $k_y$. By measuring the Uhlmann phase along $\theta$, for different values of $\delta$, we can extract the value of the winding number by observing discontinuous jumps in the Uhlmann phase.

More complicated Hamiltonians involving more qubits could be considered in a more general setup. Actually, it has been shown in Ref. [14] that an $L-$qubit interacting system can be mapped onto two types of systems that we discuss in what follows.

On the one hand, a system of 2 qubits can be mapped to a system of two interacting fermions with spin 1/2. Therefore, an Uhlmann experiment for interacting 2-qubit Hamiltonians would be the first experimental measurement of a topological phase associated to an interacting system in a mixed state. It would be very interesting

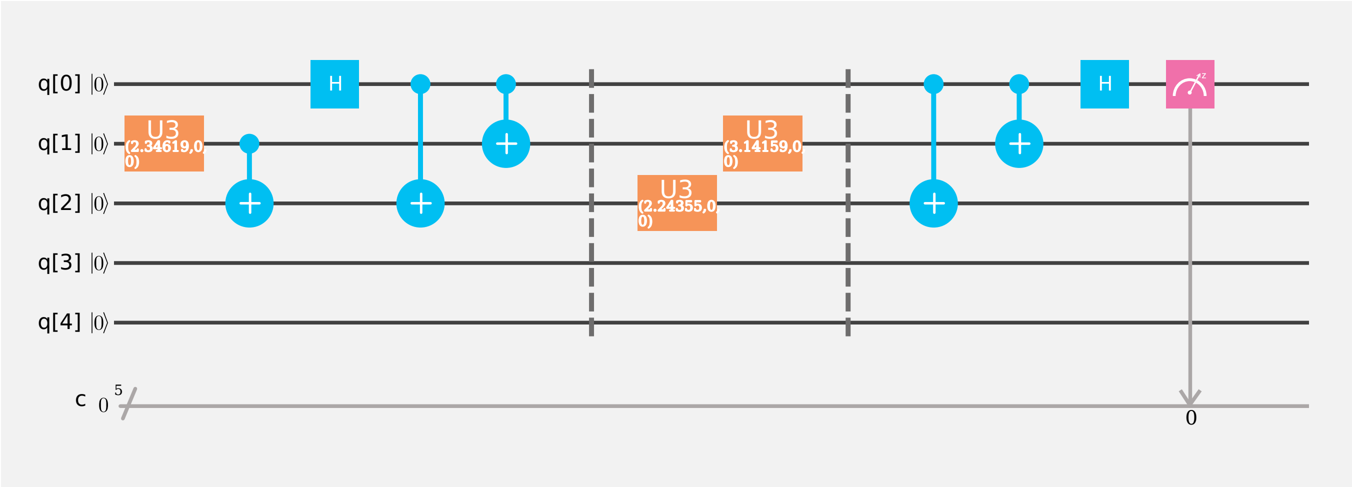


FIG. S2: Example of the circuit diagram on the IBM Quantum Experience for the measurement of the topological Uhlmann phase for $r = 0.15$. The values for the rotation angles are $\gamma = 2 \arccos(\sqrt{1-r}) = 0.7954$, $\beta_1 = \pi$ and $\beta_2 = 2\pi\sqrt{r(1-r)} =$ 2.24355

to analyse how the interaction term counteracts or enhances the effect that noise produces in the system.

On the other hand, there is a complementary mapping from a many-body interacting spin system to Haldane-like models [15] with $2^L$ bands. These are free-fermion models but the fact of having more bands opens the possibility of having higher topological quantum numbers. From the point of view of the Uhlmann theory of symmetry-protected topological order at finite temperature, one can envision the possibility of testing topological transitions between non-trivial topological phases solely driven by noise or temperature. This is an effect that only appears in systems with high topological numbers as shown in [9].

[1] A. Uhlmann, Rep. Math. Phys. **24**, 229 (1986).
[2] A. Uhlmann, Ann. Phys. (Leipzig) **46**, 63 (1989).
[3] A. Uhlmann, Lett. Math. Phys. **21**, 229 (1991).
[4] M. Hübner, Phys. Lett. A **179**, 226 (1993).
[5] A. Uhlmann, J. Geom. Phys. **18**, 76 (1996).
[6] O. Viyuela, A. Rivas and M. A. Martin-Delgado, Phys. Rev. Lett **112**, 130401 (2014).
[7] O. Viyuela, A. Rivas and M. A. Martin-Delgado, 2D Mater. **2** 034006 (2015).
[8] J. C. Budich and S. Diehl, Phys. Rev. B **91**, 165140 (2015).
[9] O. Viyuela, A. Rivas and M. A. Martin-Delgado, Phys. Rev. Lett **113**, 076408 (2014).
[10] Z. Huang and D. P. Arovas, Phys. Rev. Lett. **113**, 076407 (2014).
[11] IBM Quantum Experience `http://research.ibm.com/ibm-qx/`
[12] https://www.qiskit.org `https://www.qiskit.org`
[13] https://github.com/QISKit/openqasm `https://github.com/QISKit/openqasm`
[14] P. Roushan et al. Nature **515**, 241–244 (2014).
[15] F. D. M. Haldane, Phys. Rev. Lett. **61**, 2015 (1988).